

GEOPHYSICAL PROFILING IN SUPPORT OF A NITRATE AND URANIUM GROUNDWATER REMEDIATION STUDY

*William E. Doll, T. Jeffrey Gamey, David B. Watson, and Philip M. Jardine,
Environmental Sciences Division, Oak Ridge National Laboratory, Oak Ridge, TN*

Abstract

Multielectrode resistivity methods and pseudo-tomographic seismic refraction techniques were used to image to a depth of approximately 30m at the Field Research Center, a research site that has been developed by the U. S. Department of Energy to study bioremediation methods. The site is known to contain nitrates, uranium, and other contaminants. The geophysical methods were effective in defining the plume and in defining geologic units that appear to influence contaminant transport. Extensive drilling and groundwater sampling verified the geophysical data.

Introduction

The U. S. Department of Energy (DOE) has initiated research at the Field Research Center (FRC) on the Oak Ridge Reservation (ORR), Tennessee as part of the Natural and Accelerated Bioremediation Research (NABIR) program to develop and evaluate bioremediation tools for contaminated sites. The FRC includes a contaminated field site and an uncontaminated Background Area, both located in Bear Creek Valley (BCV) west of the Oak Ridge Y-12 National Security Complex (Figure 1). The FRC contaminated field site has been divided into 3 Areas available for NABIR researchers to conduct bioremediation field studies (Figure 2).

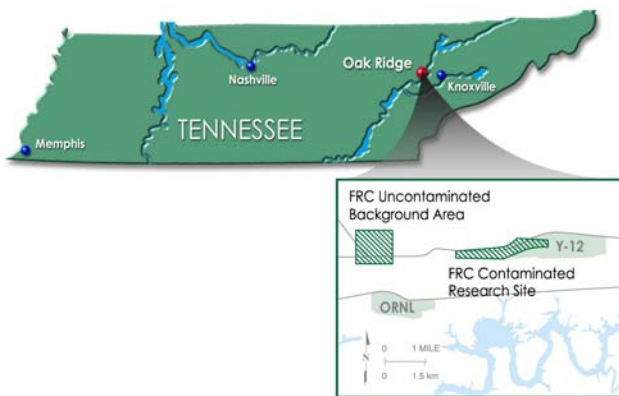


Figure 1. Location of the FRC study areas.

Liquid wastes, composed primarily of nitric acid plating wastes containing nitrate and various metals and radionuclides (e.g., uranium and technetium) were disposed of in the S-3 ponds until 1983. Waste disposal activities at the site have created a large mixed waste plume of contamination in the underlying unconsolidated saprolite and more competent shale bedrock. The ponds were neutralized and denitrified in 1984, and capped under the Resource and Conservation Recovery Act (RCRA) to reduce infiltration

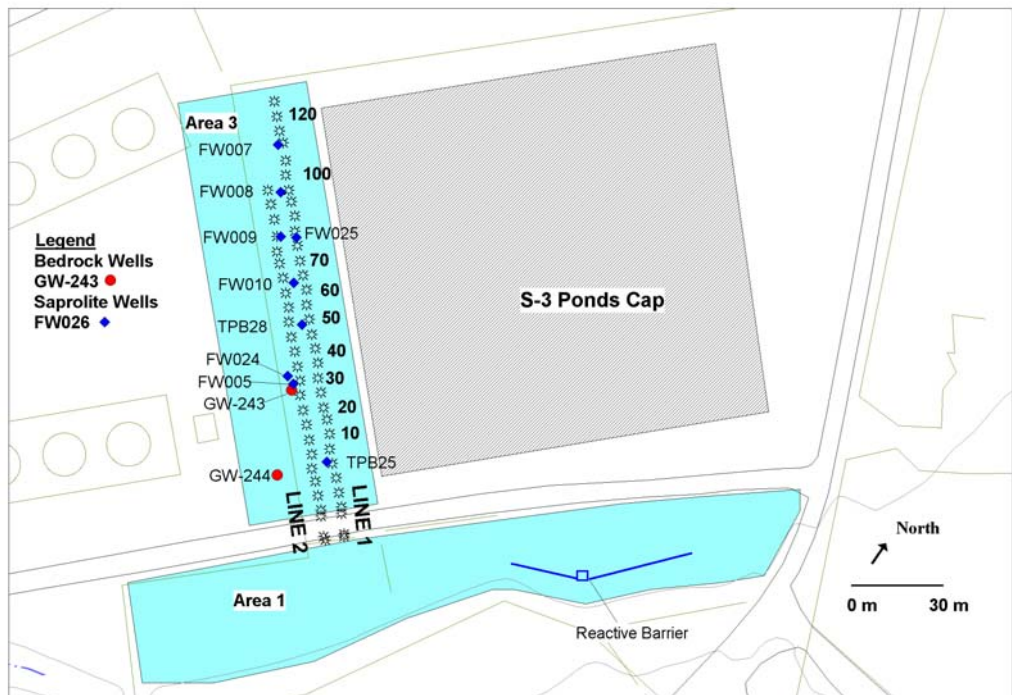


Figure 2. Site map, showing Area 3, adjacent features, and geophysical survey lines.

of rainfall and flow of contaminants into the groundwater system. A parking lot was subsequently constructed over the cap.

In order to select appropriate field scale research plots for the FRC it is beneficial to know as much as possible about the location of the plume and the geologic structures that control its distribution in three-dimensional space. Typically this information has been derived by drilling a series of expensive monitoring wells and analyzing samples at regular depth intervals within the wells. This requires that care be taken to assure that the casings are sealed, so as to prevent migration of contaminants along the well bore. Geophysical measurements were used to reduce the extent of drilling, reduce costs, and assure continuity between wells. Geophysical data were acquired in Area 3 (Figure 2) located immediately adjacent to the west side of a parking lot which was built as a cap over the former S-3 Disposal Ponds.

Background

Geology

The Nolichucky shale bedrock dips approximately 45 degrees to the southeast and has a strike of N55E (parallel to BCV) under the site. Overlying the bedrock is unconsolidated material that consists of weathered bedrock (referred to as residuum or saprolite), man-made fill, alluvium, and colluvium. Silty and clayey saprolite comprises a majority of the unconsolidated material in this area. The thickness of residuum overlying

the Nolichucky shale is typically between 5 and 15 m (15 and 50 ft) thick. Between the unconsolidated residuum and competent bedrock is a transition zone of weathered fractured bedrock. Remnant fracturing in the residuum and transition zone increases the permeability relative to the silt and clay matrix.

In the course of reviewing historical air photographs, it was reported that a small stream channel had been filled in, crossing roughly through the center of our study area. The precise location of this filled stream was not known.

Hydrogeology

The S-3 ponds are located on a hydrogeologic divide. The plume is over 400 feet deep in some areas directly beneath the ponds and extends 4,000 feet along geologic strike both east and west of the ponds. The plume may have reached these depths (in part) because the high salinity of the wastewater gave it a slightly higher density than the natural groundwater and this enhanced its downward migration along fractures and bedding planes. Total dissolved solids (TDS) content of the groundwater plume is > 60,000 mg/L in some areas near the ponds. The S-3 Ponds plume also contains elevated levels of nitrate, bicarbonate, and other ions, metals, uranium, technetium-99, and tetrachloroethylene (PCE). The plume is stratified, with the distribution of contaminants dependent on geochemical characteristics of the contaminants and groundwater. For example nitrate and technetium, which are not highly particle reactive, have the most extensive distribution in groundwater. Uranium and metals that are more reactive are not as deep and have not migrated as extensively away from the ponds

Bioremediation

NABIR FRC research projects are focused primarily on basic science research involving the use of microorganisms to bioremediate metal and radionuclide contamination in the subsurface. The focus of the NABIR research at the S-3 Ponds site is on the use of microorganisms to reduce and precipitate uranium but must also be concerned with the presence of nitrate in groundwater because it impacts the bioremediation of the other contaminants. Uranium is present in the uranyl form or U (VI). The procedure used to bioreduce uranium and nitrate involves injection of electron donors or a carbon source such as acetate or glucose.

Geophysics

To support the planned drilling and subsurface characterization effort, geophysical profile data were acquired to determine geologic structure and to detect ionic contaminants. Several geophysical techniques were considered for mapping and/or profiling the plumes and geologic units. For the initial investigation, two complementary methods were selected. Both are non-invasive methods that have, in the past 5-10 years, been extended from more conventional one-dimensional imaging counterparts to provide two-dimensional profiles of the subsurface.

To image the ionized plume components as well as geologic structures, we conducted a multielectrode resistivity survey with a Sting/Swift 56-electrode system with 1m and 2m electrode separations in both dipole-dipole and Schlumberger configurations. Processing of the resistivity data was done with AGI-2Dinv software.

Several tomographic or pseudo-tomographic seismic refraction software products are currently available for imaging geologic structures in two dimensions. Seismic methods are largely insensitive to the presence or absence of contaminants, except where their fluid properties may have subtle effects on velocity and reflectivity. They can have greater depth penetration than the multielectrode resistivity methods. These methods use dense shot patterns and large geophone arrays to provide a data set that can be inverted for velocity over a grid of points in a profile. The constant velocity and/or continuous layer restrictions of conventional delay-time or generalized reciprocal methods can thus be relaxed to yield a profile that is more representative of many near-surface environments. Seismic data were processed using Rayfract software.

Data were acquired with both systems along two north-south oriented parallel profile lines 7m apart (Figure 2). The study area is bounded to the south by a power line and small paved road. To the east (between the geophysics lines and the S-3 cap) is a small trench filled with limestone boulders, averaging about 10 cm in diameter. The parking lot bounds the east side of this trench, and is approximately 2-3m higher than the base of the trench. A chain link fence bounds the west side of the study area. One steel-cased well (GW-243) and three shallow PVC-cased sampling wells were present at the site before acquisition of the geophysical data in November and December 2001.

Geophysical Acquisition and Processing

Seismic Data Acquisition

The location of seismic shot points and receiver locations is shown in Figure 2. We acquired our data with a Bison EWG-1 bumper-mounted accelerated weight drop source, and a Geometrics Strataview 48-channel engineering seismograph using a geophone spacing of 1m. Shot points extended one-half array aperture (24m) south of the southernmost geophone, and one full array aperture to the north of the northernmost geophone. Complete data sets were acquired on Line 1 with two sets of geophones. For the first data set, Sensor Model SM-24/U-B 10 Hz geophones were used to assure accurate depth profiling by including the full suite of wavelengths up to that of the depth of interest. Data were also acquired with Mark Products model L-40A 40 Hz geophones in order to enhance the high frequency content of the recorded traces to allow first break picking to be more precise. Both sets of geophones will detect energy at or below 10 Hz, but the low frequencies will be attenuated in data acquired with 40 Hz geophones. Energy above 100 Hz can sometimes be contaminated by parasitic ringing with 10 Hz geophones. Optimal selection of geophones must also consider the source spectrum, which is rarely flat in the band of interest. Rather than conduct a detailed theoretical analysis, we chose to collect data with both sets of geophones. Data were sampled at 1/8 ms interval to allow the maximum precision in first break picking.

Seismic Processing

The seismic data recorded with the 40 Hz geophones has a consistently high signal-to-noise ratio. The waveforms were non-impulsive, so first breaks were difficult to pick. This was done with the SIPIK software package and the pick file was imported into Rayfract.

Rayfract allows two approaches to data inversion. The Delta t-V method is a pseudo-tomographic method that yields one-dimensional velocity profiles for each common midpoint (CMP). There is also an option within Rayfract for full tomographic inversion, based on the Waveform Eikonal Traveltime (WET) method (Schuster and Quintus-Bosz 1993). The Delta t-V approach fails to image sharp discontinuities in velocity with depth, or abrupt lateral variations in overburden velocity, because it assumes a dipping N-layer model below each CMP. The amount of lateral smoothing may be controlled by specifying the number of adjacent CMP positions for which CMP sorted traveltimes are stacked/binmed. The binning occurs before the 1D inversion. The WET solution does not have these restrictions. Both methods were applied to these data. Figure 6 shows the Delta t-V inversion for the southern portion of Line 1.

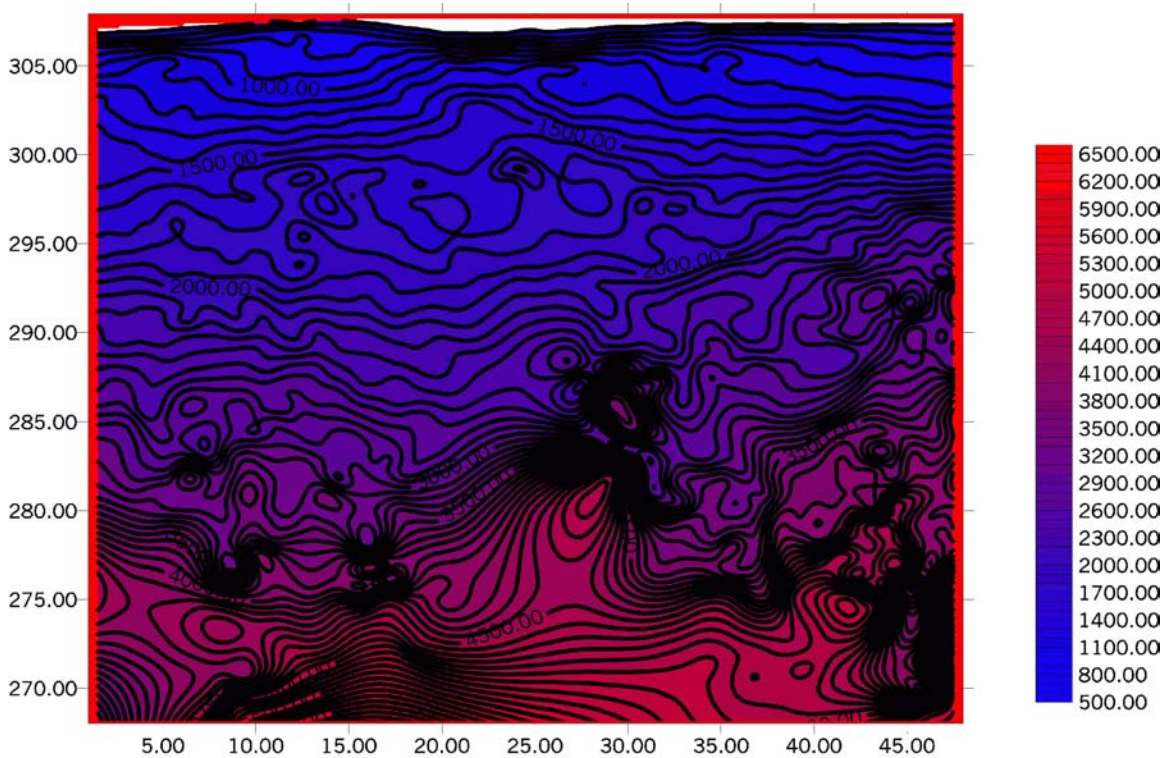


Figure 3. Delta t-V seismic velocity section for the southern portion of Line 1.

The primary region of interest for the remediation is the top 20m of the section. Selected velocity contours can be used to differentiate zones in the section. A steep velocity gradient occurs between $x=20\text{m}$ and $x=30\text{m}$ in the top 2-3m of the section where velocities increase from 500m/s to 1000 m/s and reach 1000 m/s shallower than in the adjoining portions of the section. Velocities are higher beneath this zone to a depth of about 6m (301m altitude). We associate the lateral variability in the top 3-6m as being due to differences between fill materials vs. naturally weathered rock. A lens-shaped zone of lower vertical velocity gradient and lateral velocity discontinuity occurs roughly between the 1500 m/s contour and the 2000 m/s contour. Within this region, lateral velocity changes of a few hundred m/s are common over distances of a few meters.

Between the 2000 m/s contour and the 3000 m/s or 3500 m/s contours, there is a transition to a zone of steep gradients with lateral discontinuities. This zone may represent the weathered fractured bedrock between saprolite and bedrock that is largely unweathered.

Resistivity Acquisition and Processing

Resistivity data were collected with the AGI Sting/Swift system using 56 electrodes over the same lines as the seismic system. The electrode spacing was set to 2m. Both the dipole-dipole and Schlumberger array configurations were collected, but only the dipole-dipole data are shown here. Line 1 was also surveyed in two overlapping sections using a 1m electrode spacing and a dipole-dipole configuration. Small amounts of salt water were added to each electrode location to enhance their electrical contact.

Data were recorded internally and downloaded to PC for processing using the AGI 2Dinv software. A topographic model was included in the inversion and horizontal coordinates were shifted to register with the seismic data. The second inversion iteration was chosen as the final model.

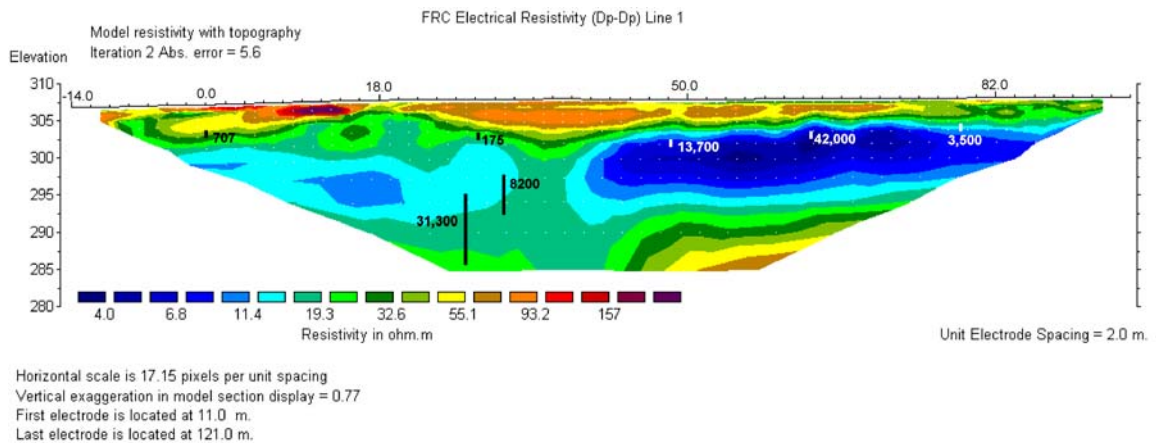


Figure 4. Multielectrode resistivity section (dipole-dipole) for Line 1. Measured nitrate concentrations (see Table 1) are superimposed on the section along with lines that depict the screen interval from which the nitrate samples were acquired.

Comparison of Seismic and Resistivity Sections

Figure 5 shows the seismic velocity contours from Figure 3 superimposed on the equivalent portion of the resistivity section from Figure 4. There are several similarities between the two results. The low velocity portions of the seismic section in the top 3-5m correspond in location and general shape with resistivities greater than 50 ohm-m in the resistivity section. The conducting region between 292 and 301m in the resistivity section shows strong correlation with the region of lateral heterogeneity bounded by the 1500m/s and 2000m/s contours in the seismic section. At depth, increases in resistivity are generally associated with increases in velocity or strong gradients in the seismic velocity. This may be an indication of unweathered bedrock.

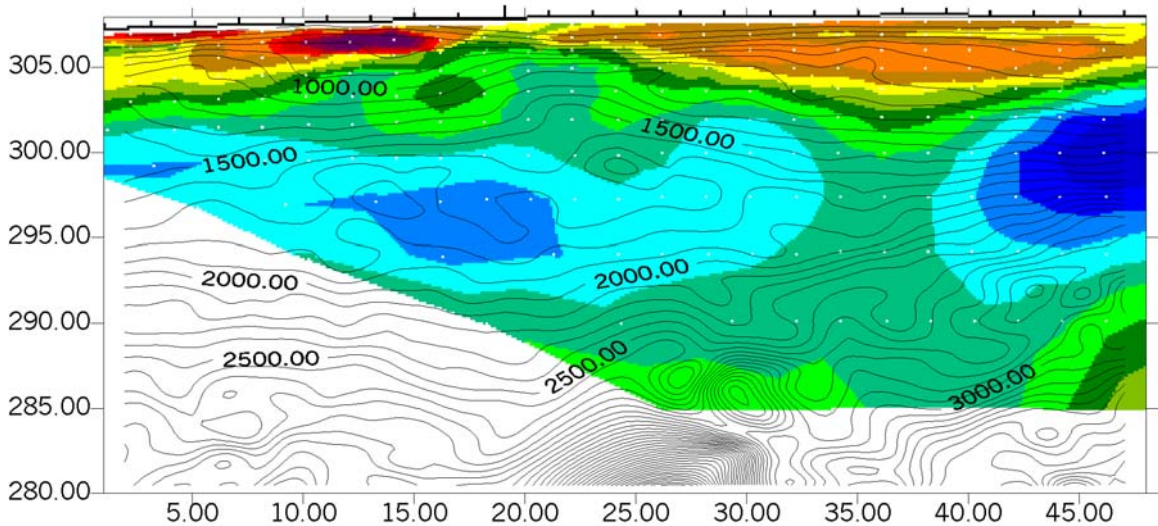


Figure 5. Integrated seismic and resistivity map for a portion of Line 1. Seismic velocity contours (from Figure 3) are overlain on the equivalent portion of the resistivity cross-section of Figure 4. Color-coding for the resistivity contours are the same as in Figure 4.

Drilling and Groundwater Sampling

The integrated seismic and resistivity data were utilized to formulate hypotheses regarding the probable areas of contaminant transport. Our intent was to locate and establish a field facility for investigating the subsurface processes that control the microbially mediated reduction, and subsequent immobilization of uranium. The resolution of the geophysical measurements was sufficient for guiding the spatial location and depth of numerous groundwater sampling wells. Seismic refraction tomography was used to estimate the vertical extent of auger penetration, while electrical resistivity was used to target subsurface regimes where elevated concentrations of uranium and NO_3^- were suspected. Three groundwater monitoring wells, namely FW010, FW024, and FW005, were situated in regimes indicative of high, moderate, and low resistivity, respectively (Fig. 4). FW024 is located immediately adjacent to FW005, but the latter samples a shallower depth. Groundwater nitrate concentrations from the three wells were found to agree extremely well with the electrical resistivity measurements where high, moderate, and low resistivity regimes contained 42000, 8000, and 175 mg/L NO_3^- , respectively (Table 1).

Groundwater geochemistry in the vicinity of FW024 was scientifically appealing and multilevel flow and chemistry monitoring were initiated. A bladder pump was situated in a straddle packer design for measuring groundwater flux via a point-dilution technique, and geochemistry as a function of depth. The results suggested that 90-95% of groundwater flow was within the 9.1 to 13.7m depth interval (298 to 293 m elevation) and that groundwater U and NO_3^- concentrations were nearly uniform from 6.1 to 13.7m. (303 to 292 m elevation). These data agreed extremely well with the geophysical measurements (Figures 3, 4, and 5). The lens of low vertical seismic velocity gradient and laterally varying velocities at 293m to 298m elevation appears to be associated with a

possible poorly consolidated zone of enhanced groundwater flow. This was consistent with groundwater flux measurements which suggested that the bulk of groundwater flow occurred within this regime. The base of this zone, which correlates roughly with the 2000 m/s velocity contour underlain by higher vertical velocity gradients, is associated with auger refusal at the weathered bedrock interface (Figs. 4 and 5). Groundwater uranium and NO₃⁻ concentrations were homogeneous from an elevation of 303 to 293 m in well FW024, with a sharp drop in concentration occurring above 303 m. Again, these results were consistent with the electrical resistivity data that showed data that showed uniform low resistivity between 302.5 and 293 m, and increasing resistivity above 302.5 m (Figs. 3 and 5). The integrated seismic and resistivity geophysical techniques provided a rapid and effective method for defining the spatial location of contaminant plumes. These techniques not only save time and money by guiding the installation of groundwater sampling wells, they also provide enhanced subsurface spatial resolution over well data such that the likelihood of missing a significant contaminant plume is reduced.

Discussion and Analysis

Table 1 shows the nitrate concentrations that were overlain on Figure 4 along with measured fluid resistivities and resistivities derived from the inverted multielectrode resistivity survey.

Table 1. Comparison of Fluid Resistivity with Sting Survey Resistivities

Well ID	Distance on Resistivity Section (m)	Depth Range (m)	Measured Nitrate Concentration (mg/l)	Measured Fluid Resistivity (Ωm)	Resistivity from Sting Survey (Ωm)
GW-244	-1	13.1-22.9	?	.36	
TPB25	0	4.6	707	1.4	26-30
GW-243	27	13.1-22.3	31,300	.32	14-22
FW005	28	5.2	175	6.2	14-22
FW024	31	15.2	8,200	.23	16.5
TPB28	48	6.1	13,700	.70	6
FW010	63	6.7	42,000	.20	3.9
FW025	77	7.6	?	.24	7.5
FW009	78	4.6	3,500	1.5	9.9
FW008	94	3.4	3,500	1.3	11
FW007	110	3.0	3,700	.78	

The measured fluid resistivities are commonly related to the effective resistivities, as measured by a multielectrode resistivity survey, by Archie's Law (Reynolds, 1997),

$$\rho = a \phi^{-m} s^{-n} \rho_w ,$$

where ρ is the effective resistivity, ρ_w is the pore fluid resistivity, s is the volume fraction of fluid-filled pores, ϕ is the porosity, and a , m , and n are constants. In effect, the matrix resistivity is considered negligible. Archie's Law may not be reliable where clay minerals are abundant (Parasnis, 1986), as in the saprolite layer. The value of n is about 2 where there more than 30% of pore space is fluid filled. Typical values for the other two constants are $0.5 \leq a \leq 2.5$ and $1.3 \leq m \leq 2.5$.

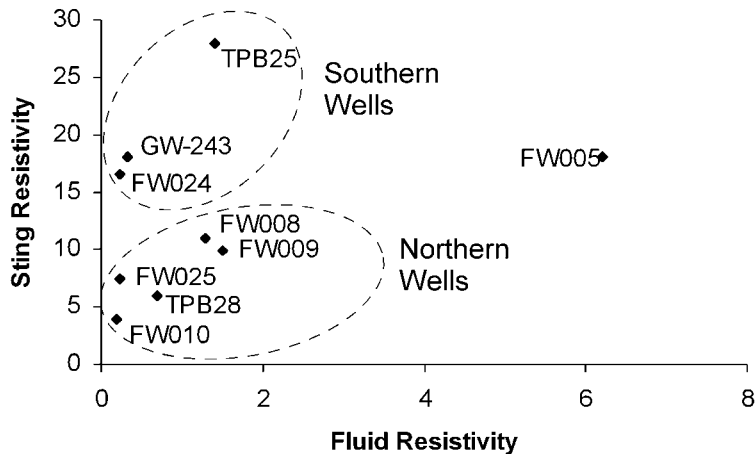


Figure 6. Plot of fluid resistivities vs. Sting resistivities from Table 1. The points can be divided into two groups, providing evidence for a fundamental change in saprolite properties between the southern area and the northern area of the profile.

Figure 6 shows the fluid resistivity values in Table 1 plotted against the corresponding resistivities derived from the relevant portion of the inverted Sting data. Taken as a whole, there is a great deal of scatter in the points. However, if the data from the three southernmost wells (TPB25, GW-243, and FW024) are separated from those from the northern wells, the two groups would fit lines with much higher correlation coefficients. We note that the southern well measurements are all from an apparent southern lobe of the plume that may be distinct from the northern lobe, as indicated by the discontinuity in the low resistivity (blue) layer at about $x=35\text{m}$. FW005 is not clearly associated with either group, though it appears that it could fall close to the projection of a line that could be fit to northern wells. It represents a sample from the shallow depth regime that could be distinct from either of the other two groups.

We interpret Figure 6 to indicate that there are at least two distinct material types at the site which differ in chemistry, porosity, pore volume, or in other properties that affect the values of the constants, a , m , and n . The differences may have to do with differences in the ratio of other ions to nitrates, clay content, differences between in situ and fill materials, differences that are associated within the mineralogy or weathering properties of the lithologies that outcrop at the site. Differences in the amounts of other ionic contaminants are known to exist between these two areas. Observations made during the drilling of these wells indicates that the material in the south tends to be more

highly leached and weathered from the migration of the acidic wastes from the S-3 Ponds. This extends to a greater depth than in the north. The northern wells are adjacent to a different pond (four ponds were covered by the cap) than the southern wells and each pond may have contained wastes of a different composition. We are assessing the impact that this might have on the geophysical data. Weathered Nolichucky shale exhibits variations in silt and clay content (Hatcher et al., 1992) that could affect its porosity or other properties along these survey lines, which are oriented perpendicular to strike. Because the beds dip at about 45°, material changes could occur over a short distance. The change in material properties might also be inferred from the seismic velocities. High velocities appear to shallow toward the north end of the seismic line (Fig. 5). This agrees with a shallower depth of refusal for push-probe wells in this area, where harder saprolite/bedrock was encountered at a shallower depth. Additional seismic work is planned to characterize the northern portion of Line 1.

Acknowledgements

We gratefully acknowledge Siegfried Rowdewald, Intelligent Resources Inc., for providing guidance in using the RAYFRAC software, and in assessing the result. Jon Nyquist (Temple University) provided guidance in using the Sting/Swift system. Barry Kinsall and Ken Lowe provided field assistance. Oak Ridge National Laboratory is managed by UT-Battelle, LLC for the U. S. Department of Energy under contract DE-AC05-00OR22725. The submitted manuscript has been authored by a contractor of the U. S. Government. Accordingly, the U. S. Government retains a nonexclusive, royalty-free license to publish or reproduce the published form of this contribution, or allow others to do so, for U. S. Government purposes.

References

- Hatcher, R.D., Jr, P. J. Lemiszki, R. B. Dreier, R. H. Ketelle, R. R. Lee, D. A. Leitzke, W. M. McMaster, J. L. Foreman, and S.Y Lee, Status Report on the Geology of the Oak Ridge Reservation, ORNL/TM-12074, Martin Marietta Energy Systems, October 1992, 244p.
- Parasnis, D. S., 1986, *Principles of Applied Geophysics*, Methuen and Co., Ltd., New York, 402p.
- Reynolds, John M., 1997, *An Introduction to Applied and Environmental Geophysics*, J. Wiley and Sons, 796 p.
- Schuster, G. T. and A. Quintus-Bosz, 1999, Wavepath eikonal traveltime inversion: Theory, *Geophysics* v. 58, p. 1314-1323 .